

High-accuracy Hg^+ microwave and optical frequency standards in cryogenic linear ion traps*

D.J. Berkeland, J.D. Miller, F.C. Cruz, J.C. Bergquist, W.M. Itano, and D.J. Wineland
*National Institute of Standards and Technology, Time and Frequency Division
Boulder, CO 80303*

We discuss time and frequency standards based on laser-cooled $^{199}\text{Hg}^+$ ions confined in a cryogenic linear rf trap. In one experiment, a 40.5 GHz source, referenced to a hydrogen maser, is servoed to the ions' ground state hyperfine transition. The stability of this clock is better than 10^{-14} using 100 s Ramsey periods, and its measured accuracy is around 10^{-13} . In a second experiment under development, a strong-binding cryogenic trap will confine a single ion used for an optical frequency standard based on the narrow $S \rightarrow D$ quadrupole transition at 282 nm. The cooling laser at 194 nm and the probe laser at 282 nm are being converted to compact, efficient, solid-state systems.

Introduction

At this workshop, groups at JPL and CSIRO describe highly stable clocks that use linear rf (Paul) traps to store buffer-gas-cooled ions [1, 2]. In these traps, most of the ions lie away from the nodal line of the trap's rf electric field. For these ions, the atomic motion driven by the oscillating trap field ("micromotion") induces significant second-order Doppler (time-dilation) shifts of the average atomic transition frequency. At NIST, our goal is to develop time and frequency standards that achieve high accuracy in addition to high stability. We confine strings of laser-cooled $^{199}\text{Hg}^+$ ions in a linear rf trap such as that depicted in Fig. 1 [3, 4]. A linear trap can confine many laser-cooled ions along the rf nodal line, where Doppler shifts and AC Stark shifts are minimum [5, 6]. Furthermore, if all the ions crystallize along the rf nodal line, there is minimal heating from the trapping fields. Thus, (perturbative) cooling laser radiation can be removed during the long probe periods of the clock transition. We use $^{199}\text{Hg}^+$, which offers a microwave clock transition at 40.5 GHz and an optical clock transition at 1.06×10^{15} Hz (see Fig. 2). To first-order, both transitions are insensitive to magnetic and electric fields at zero fields. Using linear crystals of $^{199}\text{Hg}^+$ ions, we expect to reduce all systematic shifts to less than a part in 10^{16} . If the fluctuations of the atomic signal are due only to quantum statistics, then the stability of a frequency source servoed to the atomic transition is given by [7, 8]

* Supported by ONR. Work of US Government, not subject to US copyright.

$$\sigma_y(\tau) = \frac{1}{\omega_0 \sqrt{N T_R}} \tau^{-1/2}, \quad (1)$$

where ω_0 is the frequency of the atomic transition, N is the number of ions, T_R is the Ramsey interrogation time, and τ is the averaging time of the measurement. For the ground state hyperfine transition, $\omega_0/2\pi = 40.5$ GHz. It appears feasible to use $N = 100$ ions and $T_R = 100$ s, which gives $\sigma_y(\tau) \approx 4 \times 10^{-14} \tau^{-1/2}$. For the 282 nm $5d^{10}6s^2 S_{1/2} \rightarrow 5d^9 6s^2 {}^2D_{5/2}$ electric quadrupole transition, $\omega_0/2\pi = 10^{15}$ Hz, so that using $N = 1$ and $T_R = 25$ ms gives $\sigma_y(\tau) \approx 10^{-15} \tau^{-1/2}$.

We report a preliminary evaluation of a clock based on the 40.5 GHz ground state hyperfine transition in $^{199}\text{Hg}^+$. We also discuss the development of a frequency standard based on the 282 nm electric quadrupole transition. We describe the laser systems for these experiments, and the progress towards more compact solid-state systems.

Cryogenic Linear rf Trap

Figure 1 shows the linear rf trap used in the 40.5 GHz microwave clock. Two diagonally opposite rods are held at static and rf potential ground. The potential of the other two rods is $V_0 \cos(\Omega t)$, where $V_0 \approx 150$ V and $\Omega/2\pi = 8.6$ MHz. The resulting pseudopotential confines the ions radially in a well with a secular frequency $\omega_r/2\pi \approx 230$ kHz. To confine the ions axially, two cylindrical sections at either end of the trap are held at a potential of approximately +10 V. The resulting axial potential well has a secular frequency of $\omega_z/2\pi \approx 15$ kHz. The ions are laser-cooled using the 194 nm, $5d^{10}6s^2 S_{1/2} \rightarrow 5d^{10}6p^2 P_{1/2}$ electric dipole transition shown in Fig. 2. Typically, a string of approximately ten ions is confined along the axis. By minimizing the ion micromotion in all three dimensions, we assure that the laser-cooled ions lie along the rf nodal line [9].

We place the trap in a cryogenic environment to reduce problems associated with background gas. Previously, we used a linear rf trap at room-temperature with a background pressure of approximately 10^{-8} Pa [10]. At this pressure, background neutral Hg atoms cause Hg^+ loss, presumably by forming dimers with ions excited by the cooling laser. The resulting lifetime of ions in the trap was about ten minutes. At liquid helium temperatures, however, Hg and most other background gases are cryopumped onto the walls of the chamber. In this low-pressure environment, we have trapped Hg^+ ions in the presence of laser radiation without loss for periods of over ten hours. Without laser excitation, we have confined strings of approximately ten ions for several days. With this low background pressure, most pressure shifts should be

negligible, although since helium is not efficiently cryopumped it may cause a pressure shift. Finally, operation at 4 K also reduces the shifts due to blackbody radiation. For the ground state hyperfine transition, at $T = 4$ K, the fractional blackbody Zeeman shift is -2×10^{-21} , and the fractional blackbody Stark shift is -3×10^{-24} [11]. This is significantly smaller than the fractional blackbody Stark shift for neutral cesium ($1.69(4) \times 10^{-14}$ at $T = 300$ K [11]).

Laser-atom Interactions

Laser beams at 194 nm are used for both cooling and state detection. For cooling, the $^2S_{1/2}, F = 1$ to $^2P_{1/2}, F = 0$ transition is used because it is the closest to a cycling transition (see Fig. 2). The frequency of a primary laser is resonant with this transition, but can off-resonantly excite the ion into the $^2P_{1/2}, F = 1$ level, from which the ion can decay into the $^2S_{1/2}, F = 0$ level. To maintain fluorescence, a repumping laser beam, resonant with the $F = 0$ to $F = 1$ transition, is overlapped collinearly with the primary laser beam.

To determine the atomic state, the primary beam is pulsed on for a time comparable to the time necessary to pump the ions from the $^2S_{1/2}, F = 1$ to the $^2S_{1/2}, F = 0$ level (typically 10 ms). If the ion is found in the $^2S_{1/2}, F = 1$ level, it will scatter about 10^4 photons before it optically pumps into the $^2S_{1/2}, F = 0$ level. We detect and count approximately 1% of these photons. If the transition is not saturated, the number of photons scattered before the ion is optically pumped can be made nearly insensitive to laser power. Thus the signal-to-noise ratio of the state detection signal can be limited only by “quantum projection noise” [8] if the ions are monitored individually. Currently, however, the state-detection signal is simply the combined fluorescence from all the ions. As a result, we think that fluctuations in the frequency and intensity of the 194 nm radiation, and its overlap with the ions, limit our typical stability to about twice that of Eq. (1).

The $^{199}\text{Hg}^+$ ground state Zeeman structure complicates laser cooling and state detection. For any constant laser polarization and zero magnetic field, two superpositions of the $^2S_{1/2}, F = 1, m_F = 0, \pm 1$ levels are dark states. After the ion optically pumps into these states, the fluorescence vanishes. To constantly pump the ions out of the dark states, the laser field must couple each $^2S_{1/2}, F = 1, m_F = 0, \pm 1$ level to the $^2P_{1/2}, F = 0$ level. Also, each of these three couplings must have a different time dependence. We satisfy these conditions with two non-collinear laser beams. One beam passes through a photo elastic modulator whose calcite crystal axes are tilted $\pm 45^\circ$ relative to the beam polarization. The mechanical compression along one of the crystal axes is

90° out of phase with that of the other. The resulting changes in the crystal birefringence continuously cycle the laser beam's polarization state between orthogonal circular and linear polarizations. The linear polarization of the second beam remains fixed in the plane formed by the two beams, which overlap with the ions at a 40° angle to each other.

The 40.5 GHz Microwave Clock

The measurement cycle for generating the error signal to steer the microwave frequency is as follows. First, to cool the ions, both the primary and repumping 194 nm laser beams are pulsed on for 300 ms. Next, the repumping beam is turned off for about 90 ms, so that most of the ions are optically pumped into the $^2S_{1/2}, F = 0$ level. Both beams are then blocked during the Ramsey microwave interrogation period, which consists of two 250 ms microwave pulses separated by the free precession period T_R . Finally, the primary beam is turned on for about 10 ms while we count the number of scattered photons. This determines the ensemble average of the atomic state population. The microwave frequency is alternately stepped to either side of the central Ramsey fringe at the beginning of each measurement cycle. A digital servo using a second difference algorithm [12, 13] adjusts the average frequency to maintain a constant number of fluorescence photons during each state detection step. In this way, the microwave frequency is steered to resonance with the $F = 0$ to $F = 1, m_F = 0$ ground state hyperfine transition (a 1.5×10^{-7} T magnetic field breaks the degeneracy of the $F = 1$ states). We synthesize the microwave frequency from a low-noise crystal quartz oscillator locked to an active hydrogen maser [14].

Figure 3 shows the two-sample Allan variance $\sigma_y(\tau)$ of the average microwave frequency when it is locked to the ion resonance. For averaging times τ comparable to T_R , the calculated value of $\sigma_y(\tau)$ is erroneously small, because the digital integrator has little gain at these times. As τ increases, the integral gain grows until fluctuations in the detected ion signal dominate $\sigma_y(\tau)$. Here, $\sigma_y(\tau)$ decreases as $\tau^{-1/2}$ as expected. For $T_R = 100$ s, the stability approaches the expected value of $\sigma_y(\tau) \cong 1.1 \times 10^{-13} \tau^{-1/2}$ for $\tau \gg T_R$.

For each run in which the microwave frequency is continuously servoed to the atomic transition, we average the recorded frequency. Figure 4 is a summary of the fractional deviation of the average frequencies for several runs made over nine days. The error bars are not uniform because during this time, N , T_R , the total run time τ , and other parameters were deliberately varied. The normalized value of chi-squared for this data set is 2.5, which we do not yet

understand. Although the evaluation is not yet complete, the scatter in these data indicates that our fractional accuracy is probably better than 10^{-13} .

We have begun to search for systematic effects that could shift the frequency of the microwave transition. Table 1 summarizes the present status of our measurements. We measure the average ion temperature by monitoring the width of the 282 nm transition after the cooling beams have been blocked for time T_R . This determines the second-order Doppler shift and the AC Stark shift due to the trap's rf electric fields. The width also gives an upper bound on the heating rate of the ion due to background gas (presumably helium) collisions, which is approximately proportional to the helium density n_{He} . The measured shift from helium at pressure P_{He} at room temperature is $4 \times 10^{-11} P_{He}$ (where P_{He} is in Pa) [15], or $1.6 \times 10^{-31} n_{He}$ (where n_{He} is in m^{-3}). Assuming that this shift has the same dependence on density at 4 K, the upper bound on density $n_{He} = 1.6 \times 10^{12} m^{-3}$ implies an upper bound on the fractional frequency shift of approximately 3×10^{-19} . We do not measure the temperature after each run in the present experiments. The uncertainty in the quadratic Zeeman shift is due to fluctuations and inhomogeneities in the magnetic field. We determine the average magnetic field at the site of the ions from the frequencies of the Zeeman components of the hyperfine transition. The width of these components gives an upper bound on the field inhomogeneity since the ion positions are fixed. Currents flowing in the trap electrodes may cause an rf Zeeman shift; we have searched for this shift by varying the rf power delivered to the trap. Microwave chirp may occur as the 40.5 GHz radiation is switched on and off, and is measured by varying the Ramsey precession time. Finally, we calculate shifts due to blackbody radiation [11] for ions in a 10 K environment. (We think that the background temperature is greater than 4 K due to the quartz windows in the system and power delivered to the trap.)

Optical Frequency Standard

A frequency standard with high stability can be based on the $^{199}\text{Hg}^+$ 282 nm electric quadrupole transition, which has a natural linewidth of 1.7 Hz [16]. A laser stabilized to less than 20 Hz over one minute has been locked to this transition in a single ion confined in a room-temperature rf trap [17]. With improvements to the high-finesse cavities to which the laser is locked, we expect to reduce the laser linewidth to about 1 Hz over one minute. We are developing a second cryogenic system that will house a trap for this experiment.

All Solid-state Laser Systems

To make the 194 nm and 282 nm radiation sources more compact and reliable, we are converting them to an all-solid-state design. The system we currently use to generate 194 nm light starts with radiation from a single-frequency argon-ion (Ar^+) laser at 515 nm. About 500 mW is frequency-doubled in a cavity containing a BBO crystal to produce 257 nm radiation. About 5.5 W pumps a Ti:sapphire laser to make 500 mW of 792 nm radiation. The 792 nm and 257 nm beams are each enhanced in separate optical cavities, whose foci overlap in a second BBO crystal. This creates about 100 μW of 194 nm radiation through sum-frequency mixing. The Ti:sapphire laser can be replaced by an injection-locked diode laser that produces over 500 mW of 792 nm radiation [18, 19]. The Ar^+ laser will be replaced by a 1 W single-frequency, diode-pumped, frequency-doubled Yb:YAG laser at 1.029 μm [20]. Since the doubling efficiency in KNbO_3 can be 50% [21], we expect to generate about 500 mW of 515 nm radiation.

The present system for generating 282 nm radiation consists of an Ar^+ laser pumping a dye laser that produces 500 mW of 563 nm radiation. The 563 nm light is frequency-doubled by single-passing it through a 90° phase-matched AD*P crystal to give up to 100 μW of 282 nm radiation. To convert this to a solid-state system, the dye laser and pump laser will be replaced by a diode-pumped Nd:FAP laser at 1.126 μm . Approximately 100 mW of single-frequency radiation from the Nd:FAP laser has been frequency-doubled in KNbO_3 to produce 7 mW of 563 nm radiation. The light at 563 nm can be frequency-doubled as before to generate about 2 μW of 282 nm radiation. When the light is focused to about 25 μm and there is no broadening, less than 1 pW of 282 nm light will saturate the quadrupole transition.

Summary

We have locked a synthesizer to the 40.5 GHz transition in laser-cooled strings of $^{199}\text{Hg}^+$ ions in a linear cryogenic rf trap. With Ramsey periods of up to 100 s, this clock has demonstrated stabilities of better than 10^{-14} . Preliminary investigations of systematic frequency shifts indicate an accuracy of better than 10^{-13} . In the future, we plan to use Ramsey times of 100 s and a smaller, more tightly confining trap that stores up to 100 ions. We will soon resume work on a cryogenic 282 nm optical frequency standard, whose potential stability is $\sigma_y(\tau) \approx 10^{-15} \tau^{-1/2}$. Finally, we are converting our laser systems to an all-solid-state design, which should allow longer continuous running times.

References

- 1 R.L. Tjoelker, J.D. Prestage, and L. Maleki, in Proc. of the Fifth Symp. Freq. Standards and Metrology, ed. James C. Bergquist, 33 (World Scientific, 1996).
- 2 Peter T.H. Fisk, Mathew J. Sellars, Malcolm A. Lawn, and Colin Coles, in Proc. of the Fifth Symp. Freq. Standards and Metrology, ed. James C. Bergquist, 27 (World Scientific, 1996).
- 3 M.E. Poitzsch, J.C. Bergquist, W.M. Itano, and D. J. Wineland, *Rev. Sci. Instrum.* **67**, 129 (1996).
- 4 J.D. Miller, D.J. Berkeland, F.C. Cruz, J.C. Bergquist, W.M. Itano, and D.J. Wineland, in 1996 IEEE International Frequency Control Symposium, 1086 (1996)
- 5 H.G. Dehmelt, in Frequency Standards and Metrology, ed. A. DeMarchi. Berlin: Springer, 286 (1989).
- 6 J.D. Prestage, G.J. Dick, and L. Maleki, *J. Appl. Phys.* **66**, 1013 (1989).
- 7 D.J. Wineland, Wayne M. Itano, J.C. Bergquist, J.J. Bollinger, F. Diedrich, and S.L. Gilbert, Proc. 4th Symposium on Freq. Standards and Metrology, Ancona, Italy, Sept. 1988; ed. A. Demarchi (Springer Verlag, Heidelberg).
- 8 W.M. Itano, J.C. Bergquist, J.J. Bollinger, J.M. Gilligan, D.J. Heinzen, F.L. Moore, M.G. Raizen, and D.J. Wineland, *Phys. Rev. A* **47**, 3554 (1993).
- 9 D.J. Berkeland, J.D. Miller, J.C. Bergquist, W.M. Itano, and D.J. Wineland, (unpublished).
- 10 M.G. Raizen, J.M. Gilligan, J.C. Bergquist, W.M. Itano, and D.J. Wineland, *Phys. Rev. A* **45**, 6493 (1992).
- 11 Wayne M. Itano, L.L. Lewis, and D.J. Wineland, *Phys. Rev. A* **25**, 1233 (1982).
- 12 Leonard S. Cutler, Robing P. Giffard, and Michael D. McGuire, Proc. 13th Ann. PTTI Meeting, 563 (1981).
- 13 J.D. Prestage, G.J. Dick, and L. Maleki, Proc. 19th Ann. PTTI Meeting, 285 (1987).
- 14 C.W. Nelson, F.L. Walls, F.G. Ascarrunz, and P.A. Pond, in 1992 IEEE Frequency Control Symposium, 64 (1992)
- 15 L.S. Cutler, R.P. Giffard, and M.D. McGuire, in Proc. 37th Ann. Symp. Freq. Contr., 32 (1983).
- 16 J.C. Bergquist, F. Diedrich, Wayne M. Itano, and D.J. Wineland, in Laser Spectroscopy IX, ed. by M.S. Feld, J.E. Thomas, and A. Mooradian, 274 (Academic, San Diego, 1989).
- 17 J.C. Bergquist, W.M. Itano, and D.J. Wineland, Frontiers in Laser Spectroscopy, 357 (1994).
- 18 D.J. Berkeland, F.C. Cruz, and J.C. Bergquist, submitted to *Appl. Opt.*
- 19 F.C. Cruz, M. Rauner, J.H. Marquardt, L. Hollberg, and J.C. Bergquist, in Proc. of the Fifth Symp. Freq. Standards and Metrology, ed. James C. Bergquist, 511 (World Scientific, 1996).
- 20 P. Lacovara, H.K. Choi, C.A. Wang, R.L. Aggarwal, and T.Y. Fan, *Opt. Lett.* **16**, 1089 (1991).
- 21 Z.Y. Ou, S.F. Pereira, E.S. Polzik, and H.J. Kimble, *Opt. Lett.* **17**, 640 (1992).

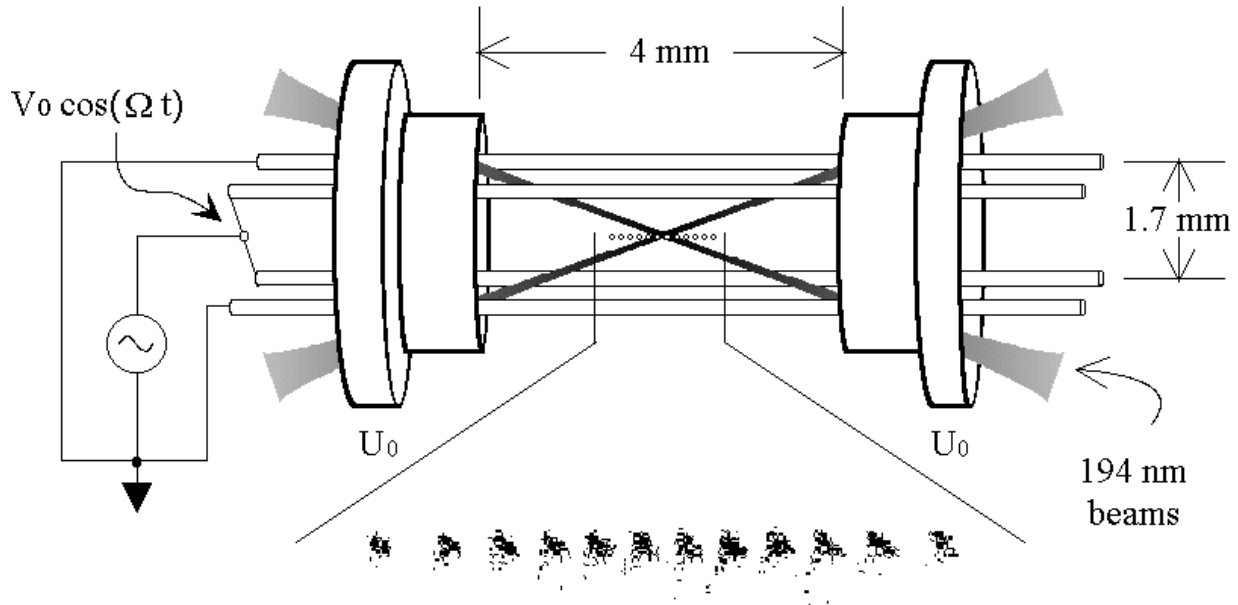


Figure 1: Linear rf trap, and an image of a string of twelve ions. The ions are spaced approximately $10 \mu\text{m}$ apart. The spatial extent of the ions is exaggerated for clarity; in reality the laser beams overlap all of the ions.

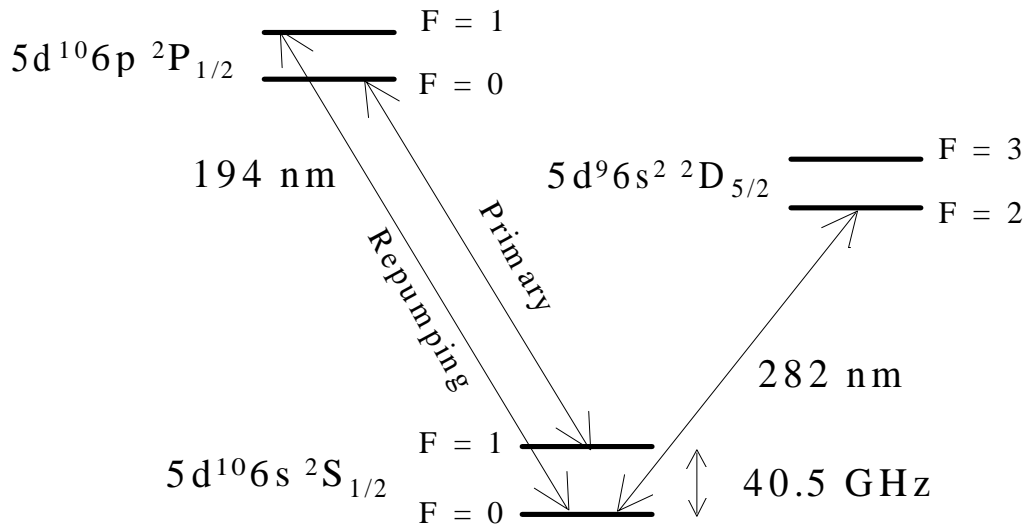


Figure 2: Partial energy diagram of $^{199}\text{Hg}^+$. The 70 MHz wide 194 nm transition is used for laser cooling and detection. The 40.5 GHz and 282 nm transitions are the clock transitions.

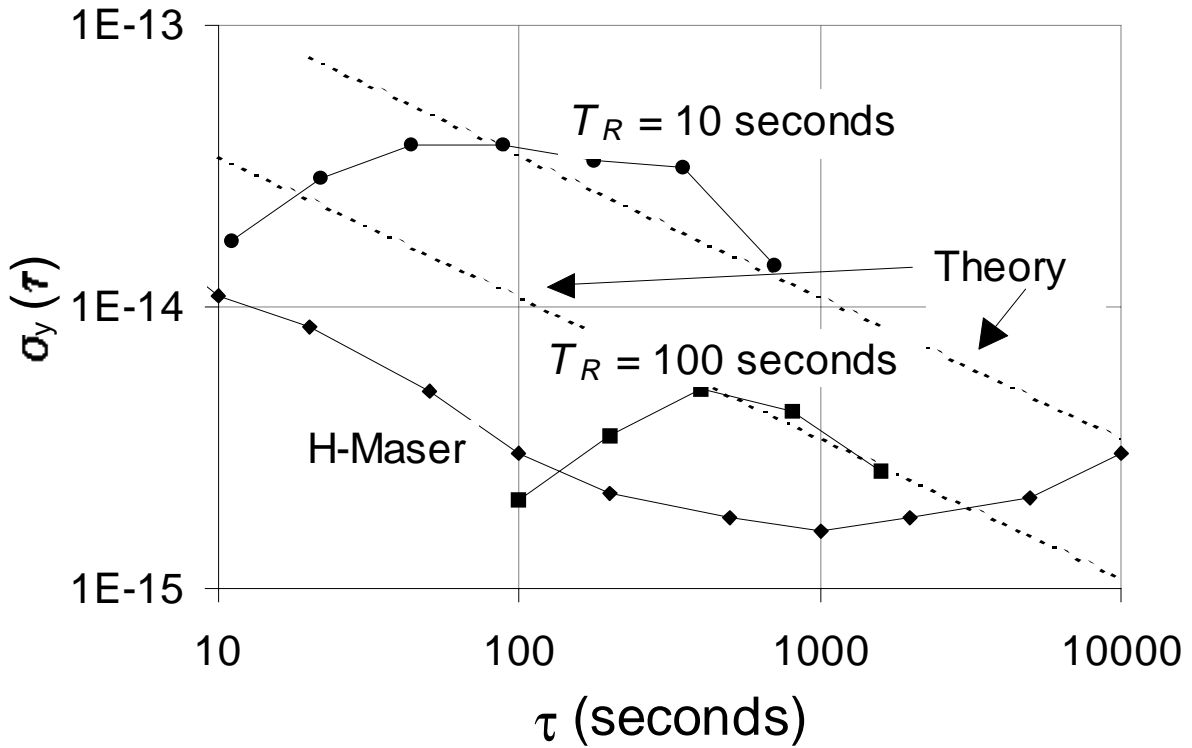


Figure 3: Stability plots for the 40.5 GHz microwave clock, using $N = 13$ ions, and both $T_R = 10$ s and $T_R = 100$ s. Also shown are the theoretically expected stabilities from Eq. (1), and the stability of the hydrogen maser reference clock.

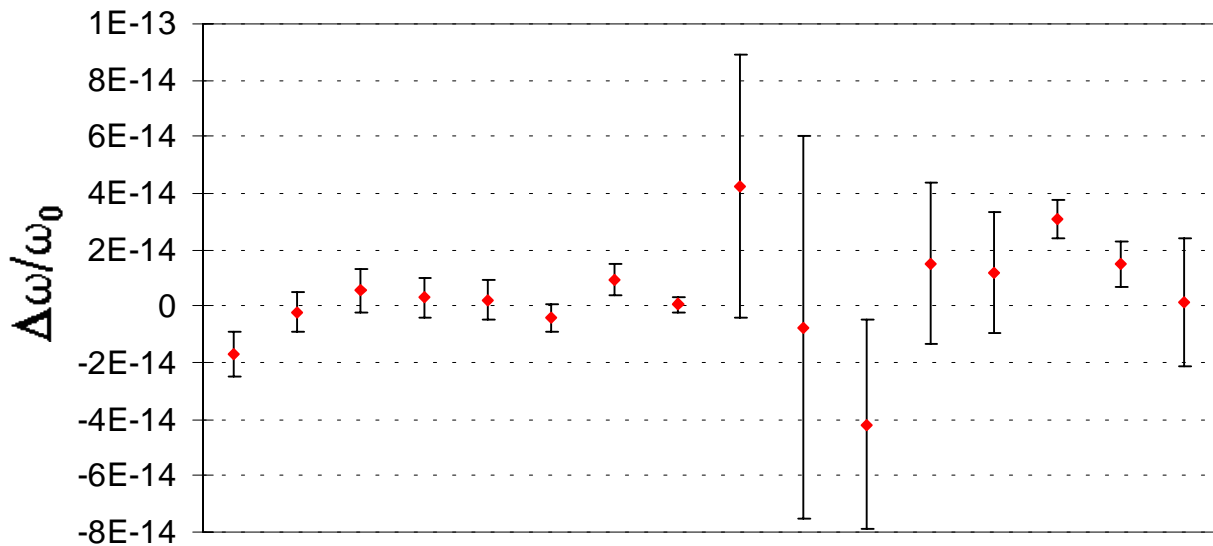


Figure 4: Summary of average frequencies over a nine-day period. The frequencies are plotted in the order in which they were measured, but the spacing of the data points does not otherwise correspond to the time in which the data were taken.

Shift	Scaling	Uncertainty
Second-order Doppler	$-\langle V^2/c^2 \rangle$	1.6×10^{-17}
Quadratic Zeeman (static)	$+\langle B^2 \rangle$	3×10^{-15}
Quadratic Zeeman (rf)	$+\langle B^2 \rangle$	3×10^{-14}
AC Stark (rf)	$-\langle E_{rf}^2 \rangle$	3×10^{-18}
Microwave chirp	$1/T_R$	3×10^{-15}
He pressure shift	n_{He}	3×10^{-19}
Blackbody AC Zeeman ($T = 10$ K)	$-T^2$	1.4×10^{-20}
Blackbody AC Stark ($T = 10$ K)	$-T^4$	1.2×10^{-22}

Table 1: Measured uncertainties in the microwave clock. Effects below the dashed line are expected to be negligible compared to those above the dashed line.